

The contribution of fungal spores and bacteria to regional and global aerosol number and ice nucleation immersion freezing rates

Spracklen, D. V.¹ & Heald, C. L.²

[1] {School of Earth and Environment, University of Leeds, Leeds, UK. }

[2] {Department of Civil and Environmental Engineering, Massachusetts Institute of Technology, Cambridge, MA, USA. }

Correspondence to: D. V. Spracklen (dominick@env.leeds.ac.uk)

Abstract

Primary biological aerosol particles (PBAP) may play an important role in aerosol-climate interactions, in particular by affecting ice formation in mixed phase clouds. However, the role of PBAP is poorly understood because the sources and distribution of PBAP in the atmosphere are not well quantified. Here we include emissions of fungal spores and bacteria in a global aerosol microphysics model and explore their contribution to concentrations of supermicron particle number, cloud condensation nuclei (CCN) and immersion freezing rates. Simulated surface annual mean concentrations of fungal spores are $\sim 2.5 \times 10^4 \text{ m}^{-3}$ over continental midlatitudes and $1 \times 10^5 \text{ m}^{-3}$ over tropical forests. Simulated surface concentrations of bacteria are $2.5 \times 10^4 \text{ m}^{-3}$ over most continental regions and $5 \times 10^4 \text{ m}^{-3}$ over grasslands of central Asia and North America. These simulated surface number concentrations of fungal spores and bacteria are broadly in agreement with the limited available observations. We find that fungal spores and bacteria contribute 8% and 5% respectively to simulated continental surface mean supermicron number concentrations, but have very limited impact on CCN concentrations, altering regional concentrations by less than 1%. In agreement with previous global modelling studies we find that fungal spores and bacteria contribute very little (3×10^{-3} % even when we assume upper limits for ice nucleation activity) to global average immersion freezing ice nucleation rates, which are dominated by soot and dust. However, at lower altitudes (400hPa to 600 hPa), where warmer temperatures mean that soot and dust may not nucleate ice, we find that PBAP controls the immersion freezing ice nucleation rate. This demonstrates that PBAP can be of regional importance for IN formation, in agreement with case study observations.

1 Introduction

Primary biological aerosol particles (PBAP) include a wide range of biological particles emitted directly from the biosphere including bacteria, viruses, fungal spores, pollen and leaf debris. It has been suggested that PBAP can make a large contribution to atmospheric aerosol (Jaenicke, 2005), influencing climate through scattering and absorbing radiation (the aerosol direct effect) and by altering the properties of clouds (the aerosol indirect effect). However, the impact of PBAP on climate is poorly constrained. Here we quantify the contribution of

38 fungal spores and bacteria to global and regional aerosol number, cloud condensation nuclei
39 (CCN) and immersion freezing rates.

40 The amount of PBAP emitted into the atmosphere is thought to be substantial with estimates
41 as large as 1000 Tg a⁻¹ (Jaenicke, 2005). Previous estimates of the global emission of fungal
42 spores vary from 8-186 Tg a⁻¹ (Elbert et al., 2007; Heald and Spracklen, 2009; Jacobson and
43 Streets, 2009; Hoose et al., 2010b; Sesartic and Dallafior, 2011; Després et al., 2012). The
44 global emissions of bacteria are even more uncertain, spanning nearly two orders of
45 magnitude from 0.4-28.1 Tg a⁻¹ (Burrows et al., 2009b; Hoose et al., 2010b; Jacobson and
46 Streets, 2009; Després et al., 2012).

47 The majority of PBAP are thought to be emitted at supermicron sizes (dry diameter > 1 µm),
48 with bacteria having diameter of about 1 µm, fungal spores 2-10 µm and pollen 30 µm
49 (Després et al., 2012). As such, PBAP may constitute an important fraction of the number
50 concentration of supermicron particles, especially when other supermicron aerosol (e.g., dust
51 and sea spray) are absent (Després et al., 2012). Over the Amazon rainforest, PBAP
52 contributes up to 80% (Pöschl et al., 2010) of total supermicron number concentrations.
53 Huffman et al. (2012) reported that fluorescent biological aerosol particles (FBAP)
54 contribute 24% of supermicron number concentrations over the Amazon. Observations over
55 Europe and central Asia show that PBAP can make up 20-30% of the number concentration
56 of particles with diameter > 0.2 µm (Matthias-Maser and Jaenicke, 1995; Matthias-Maser et
57 al. 2000), whilst other studies have found a smaller (4%) contribution of FBAP to
58 supermicron number over Europe (Huffman et al., 2010). PBAP can also make substantial
59 contributions to supermicron particle number in the free and upper troposphere. DeLeon-
60 Rodriguez et al. (2013) reported that bacteria can represent 20% of total particles in the 0.25
61 – 1 µm diameter range at ~10 km over the Atlantic Ocean.

62 PBAP are typically considered to be efficient CCN (Bauer et al., 2003; Després et al., 2012).
63 The low PBAP number concentrations are likely to limit the contribution of PBAP to total
64 CCN concentrations in most parts of the atmosphere. However, PBAP may have a role as
65 giant (> 2µm) CCN, forming cloud droplets at low supersaturations (Möhler et al., 2007;
66 Després et al., 2012).

67 PBAP may also act as ice nuclei (IN) (Möhler et al., 2007; Després et al., 2012; Murray et al.,
68 2012). Detailed aerosol-cloud models have shown that bacteria can alter the properties of
69 clouds if present in sufficiently high number concentrations (Phillips et al., 2009). Recent
70 atmospheric measurements have observed the presence of PBAP in precipitation (Christner et
71 al., 2008) and shown that IN over both the continental US (Pratt et al., 2009) and the Amazon
72 (Prenni et al., 2009) are composed of biological particles. Prenni et al. (2009) measured IN (<
73 2 µm diameter) with a continuous flow diffusion chamber and demonstrated that
74 carbonaceous material, dominated by biological particles, make up 16-76% of IN in the
75 Amazon basin during the wet season. Pratt et al. (2009) found that biological particles
76 comprised ~33% of ice-crystal residues (< 1.2 µm diameter) measured at 8 km altitude over
77 the continental United States. Observed correlations between PBAP and IN concentrations
78 during rain events over the continental United States, further suggest an important role for

79 PBAP in the hydrological cycle (Huffman et al., 2013; Prenni et al., 2013). In contrast, recent
80 modelling studies have found that PBAP make little contribution to global ice nucleation
81 (Hoose et al., 2010a;b; Sesartic et al., 2013). For example, Hoose et al. (2010b) simulated that
82 PBAP contribute less than 0.6% to the global average ice nucleation rate. However, these
83 previous global studies have not quantified the regional contribution of PBAP to ice
84 nucleation which could be higher in areas of biological activity (e.g., over tropical forests)
85 and in warm air masses (e.g., above $\sim -15^{\circ}\text{C}$). Here we use a global aerosol microphysics
86 model to quantify the contribution of fungal spores and bacteria to regional and global
87 aerosol and ice nucleation.

88 **2 Methods**

89 **2.1 Model description**

90 We used the modal version of the Global Model of Aerosol Processes (GLOMAP-mode)
91 (Mann et al., 2010) which is an extension to the TOMCAT global 3-D chemical transport
92 model (Chipperfield, 2006). The model is forced by analyses from the European Centre for
93 Medium Range Weather Forecasts (ECMWF), updated every 6 hours and linearly
94 interpolated onto the model time-step. We ran the model for the year 2000 (after 3 months
95 model spin-up) at a horizontal resolution of $\sim 2.8^{\circ} \times 2.8^{\circ}$ with 31 vertical levels between the
96 surface and 10 hPa.

97
98 GLOMAP-mode simulates aerosol component mass and number concentration (two-moment
99 modal) in 7 lognormal modes: hygroscopic nucleation, Aitken, accumulation and coarse
100 modes plus a non-hygroscopic Aitken, accumulation and coarse modes. The aerosol
101 components simulated are sulfate, sea-salt, black carbon, particulate organic matter (POM)
102 and dust. GLOMAP includes representations of nucleation, particle growth via coagulation,
103 condensation and cloud processing, wet and dry deposition and in/below cloud scavenging.
104 Mann et al. (2012) demonstrated that the modal version of GLOMAP simulates very similar
105 aerosol compared to the sectional version of the same model (Spracklen et al., 2005).

106 In this work we implemented fungal spore and bacteria emissions into GLOMAP. We used
107 emissions of fungal spores from the empirically optimised scheme of Heald and Spracklen
108 (2009), where emissions are driven by leaf area index (LAI) and atmospheric water vapour
109 concentrations. We apply the fine and coarse mode emissions calculated by Heald and
110 Spracklen (2009), assuming that the fine mode are emitted with a diameter of $1.25\ \mu\text{m}$ and
111 the coarse mode are emitted at $6.25\ \mu\text{m}$. For bacteria emissions we followed Hoose et al.
112 (2010b) which itself is based on Burrows et al. (2009b). Burrows et al. (2009b) used
113 observations of bacteria number concentration synthesised from the literature (Burrows et al.,
114 2009a) to estimate ecosystem- dependent fluxes. We applied ecosystem-dependent bacteria
115 emission fluxes to match the upper emission estimate in Hoose et al. (2010b): oceans $226\ \text{m}^{-2}\text{s}^{-1}$,
116 crops $1578\ \text{m}^{-2}\text{s}^{-1}$, forests $187\ \text{m}^{-2}\text{s}^{-1}$, grasslands $1811\ \text{m}^{-2}\text{s}^{-1}$, shrubs $619\ \text{m}^{-2}\text{s}^{-1}$, tundra
117 $579\ \text{m}^{-2}\text{s}^{-1}$, desert/land-ice $52\ \text{m}^{-2}\text{s}^{-1}$. We used the MODIS International Global Biosphere
118 Programme (IGBP) global land cover classification to determine the spatial distribution of
119 different ecosystems. We mapped ecosystem types defined by Burrows et al. (2009a) onto

120 MODIS IGBP land cover classifications, weighting the emission flux by the area fraction of
121 each ecosystem as determined by MODIS. The global average annual mean land-surface
122 bacteria emission flux is $410 \text{ m}^{-2}\text{s}^{-1}$ in our implementation, which is similar to the $380 \text{ m}^{-2}\text{s}^{-1}$
123 reported by Burrows et al. (2009a). Note the emission scheme for bacteria does not include a
124 dependence on LAI. We used an emission diameter of $1 \mu\text{m}$ for bacteria as used by previous
125 studies (Hoose et al., 2010a). We assumed that both bacteria and fungal spores are composed
126 of POM, are hydrophilic on emission (Heald and Spracklen, 2009) and are emitted into the
127 hygroscopic modes. Other global model studies (e.g., Sesartic et al., 2013) have assumed that
128 fungal spores are hydrophobic on emission, with this assumption extending the simulated
129 lifetime of PBAP.

130 CCN concentrations were calculated using the simulated aerosol size distribution and the
131 approach of Petters and Kreidenweis (2007). We assign hygroscopicity parameters for
132 sulphate (0.61, assuming ammonium sulfate), sea salt (1.28), black carbon (0.0), and POM
133 (0.1). To calculate the potential contribution of PBAP to ice nucleation we quantified the
134 contribution of different aerosol sources (dust, soot, bacteria and fungal spores) to immersion
135 freezing rates: the dominant heterogeneous ice nucleation pathway in mixed-phase clouds
136 (Hoose et al., 2010a). We calculate immersion freezing rates using the parametrization of
137 Hoose et al. (2010a; b) which is based on classical nucleation theory and laboratory
138 experiments. As in Hoose et al. (2010a; b) we assumed that only 0.1% of fungi and bacteria
139 and 1% of soot have the potential to be IN active. No upper limit is applied for dust (100% of
140 particles can act as IN). The potential of PBAP to nucleate ice is uncertain (Murray et al.,
141 2012), so we carried out a sensitivity study where we assumed that all PBAP can be IN active
142 with no upper limits for IN formation from PBAP. This simulation matches the PBAP-max
143 simulation in Hoose et al. (2010a; b). We report immersion freezing rates in two ways: all sky
144 and weighted by ice-cloud fraction. We apply monthly mean ice cloud fraction from the
145 International Satellite Cloud Climatology Project (ISCCP) D2 data (Rossow and Schiffer,
146 1999) for the year 2000.

147

148 **2.2 PBAP observations**

149 We compared simulated PBAP number concentrations against observations synthesised from
150 the literature. Observations of the number concentration of PBAP in the atmosphere are
151 limited, long-term observations are rare and there are specific measurement issues. For
152 example, many studies report the number of culturable fungi or bacteria, despite the fact that
153 this method only accounts for a fraction of the total number (Burrows et al., 2009a). For
154 bacteria, the fraction of total bacteria which are cultural can be as low as 1% (Burrows et al.,
155 2009a). Furthermore, most observational techniques rely on manual counting, a method that
156 is subject to significant operator bias.

157 We used two previous studies that had synthesised observations of the number concentrations
158 of fungal spores (Sesartic & Dallafior, 2011) and bacteria (Burrows et al., 2009a) in surface
159 air. Sesartic & Dallafior (2011) synthesised observations of fungal spores from both
160 culturable and culture-independent techniques. We report the mean, maximum and minimum

161 of the observations. Burrows et al. (2009a) synthesised observations of number concentration
162 of bacteria, applying scaling factors to convert culturable to total bacteria concentrations.
163 They give a best estimate as well as an upper and lower bounds through which they attempt
164 to account for uncertainty in both culturable bacteria number concentration as well as the
165 ratio of total to culturable bacteria. Both studies report number concentrations as a function of
166 broad ecosystem types (forest, shrub, grassland, crop, tundra). We used the IGBP land cover
167 classification from MODIS to sample the model in a similar manner.

168 To further evaluate fungal spore number concentrations we synthesised observations of long-
169 term (those with at least a full annual cycle) fungal spore number concentrations from the
170 literature (Ho et al., 2005; Sousa et al., 2008; Grinn-Gofron et al., 2011; Herrero et al., 2006;
171 Lim et al., 1998; Henriquez et al., 2001; Hasnain et al., 2012). Observations are typically
172 made using 7-day spore traps and microscopic identification and counting techniques; these
173 methods are inherently uncertain and subject to operator error. Observations are available in
174 both hemispheres and are primarily located in urban regions.

175 **3 Results**

176 We compare our calculated global annual mean mass burden of fungal spores and bacteria to
177 that previously reported using the same PBAP emission schemes. The simulated global
178 annual mean burden of fungal spores calculated here (0.15 Tg) matches that previously
179 reported using GEOS-Chem (0.18 Tg) (Heald and Spracklen, 2009) and CAM-Oslo (0.094
180 Tg) (Hoose et al., 2010b). The simulated global annual mean burden of bacteria calculated
181 here (0.011 Tg) is also similar to previously reported by Burrows et al. (2009b) (0.0087 Tg)
182 and simulated using CAM-Oslo (0.0043 Tg) (Hoose et al., 2010b).

183 Figure 1 shows simulated surface annual mean number concentrations of fungal spores and
184 bacteria. GLOMAP-mode simulates similar continental surface mean number concentrations
185 for both fungal spores ($2.4 \times 10^4 \text{ m}^{-3}$) and bacteria ($1.9 \times 10^4 \text{ m}^{-3}$), but with different spatial
186 patterns. Simulated concentrations of fungal spores are typically $2 \times 10^4 \text{ m}^{-3}$ over mid-latitude
187 continental regions and exceed $1 \times 10^5 \text{ m}^{-3}$ over tropical forests matching the regions of
188 greatest fungal spore emission (Heald & Spracklen, 2009). Simulated surface concentrations
189 of bacteria are typically $2 \times 10^4 \text{ m}^{-3}$ over most continental regions, but are greater over
190 grassland regions of central Asia and North America where concentrations of $5 \times 10^4 \text{ m}^{-3}$ are
191 more typical. Simulated concentrations of bacteria are lower over tropical forest regions than
192 over other continental regions due to low emission flux assumed for these ecosystems
193 combined with rapid wet deposition. Over oceans, annual mean concentrations of bacteria
194 ($7.8 \times 10^3 \text{ m}^{-3}$) are substantially greater than fungal spores ($1.9 \times 10^3 \text{ m}^{-3}$), since we apply an
195 ocean flux of bacteria but no such flux for fungal spores. The global mean ratio of continental
196 surface number concentration to marine surface number concentration is 2.5 for bacteria and
197 12 for fungal spores. The magnitude and spatial distribution of our simulated bacteria number
198 concentrations is similar to that simulated by Burrows et al. (2009b).

199 Figure 2 compares simulated number concentrations of fungal spores and bacteria in surface
200 air against observations (Sesartic & Dallafior, 2011; Burrows et al., 2009a). Both studies

201 report observed number concentration as a function of ecosystem type. We used the MODIS
202 IGBP land cover classification to sample the model in a similar manner to that of the
203 observational studies. Observed fungal spore concentrations are typically $\sim 1 \times 10^4 \text{ m}^{-3}$. Fungal
204 spore number concentrations are simulated to within a factor of 3 over shrub, grassland and
205 crop ecosystems. Over forests, the model overpredicts observed concentrations of fungal
206 spores. Limiting the observational dataset to culture independent techniques (Sesartic &
207 Dallafior, 2011), increases observed concentrations by only 40% on average and is not
208 sufficient to explain the model bias. It is possible that the linear dependence of emission flux
209 on LAI applied by Heald and Spracklen (2009) is too strong, or that the particle size we apply
210 over these ecosystems is too small. Additional observations over tropical ecosystems are
211 required to explore this further.

212 Bacteria number concentrations simulated by the model reasonably match (within a factor 2)
213 observed number concentrations over ocean, desert/ice and tundra environments, but are
214 underpredicted by a factor 2-4 over forests, grasslands and crops (Fig. 2b). Given that we are
215 employing bacteria emissions from Burrows et al. (2009b) which are based on these
216 observations, good agreement for bacteria is expected. Poor understanding of the seasonal
217 cycle in emissions (Burrows et al. 2009a; Hoose et al., 2010b), combined with the limited set
218 of observations preclude a more quantitative comparison.

219 To further evaluate simulated fungal spore number concentrations we compared against long-
220 term observation of fungal spore number (Fig. 3). The model reasonably captures (within a
221 factor 2) observed annual mean number concentrations at some sites (Taiwan, Portugal, Spain
222 and Chile), but overpredicts at other locations (Poland and Singapore). As a mean across all
223 sites, simulated annual mean number concentrations are biased high (normalised mean bias
224 (NMB) = 52%), driven by the high model bias for Singapore. Despite this bias, the model
225 typically captures the observed seasonal cycle at northern hemisphere (NH) mid-latitude sites
226 with greater number concentrations during the summer as observed (Tong & Lighthart, 2000;
227 Yttri et al., 2011; Bowers et al., 2013).

228 We calculated the simulated contribution of fungal spores and bacteria to total supermicron
229 number concentrations. Previous model evaluations have demonstrated GLOMAP reasonably
230 simulates the mass and number concentrations of dust (Manktelow et al., 2010) and sea spray
231 (Mann et al., 2012), giving us confidence in the distribution of other supermicron particle
232 sources. Fungal spores are simulated to contribute 8% of annual mean continental surface
233 supermicron number concentrations. The contribution is typically $\sim 25\%$ over much of the
234 continental NH midlatitudes matching observed contributions in these regions (Matthias-
235 Maser and Jaenicke, 1995; Matthias-Maser et al. 2000). Over tropical forest regions we
236 simulate that fungal spores contribute up to 50% of supermicron number concentrations (Fig.
237 1b), similar to the large observed contribution (Pöschl et al., 2010; Huffman et al., 2012).
238 Bacteria have a smaller simulated contribution to surface supermicron number
239 concentrations, contributing 5% to continental mean supermicron number concentrations,
240 with a maximum contribution of 25% over parts of North America, boreal Asia and southern
241 Africa (Fig. 1d). Over the oceans, where sea spray dominates supermicron aerosol number

242 and the PBAP emission flux is smaller, the contribution of PBAP is small (surface ocean
243 mean of 0.4% for fungal spores and 1% for bacteria).

244 Figure 4 shows simulated zonal annual mean number concentrations of fungal spores and
245 bacteria, exhibiting similar patterns to previous studies (Hoose et al., 2010b; Sesartic et al.,
246 2013). Hoose et al. (2010a; b) apply a similar mass emission of fungal spores compared to
247 our study but assume a larger emission diameter (they emit all spores at 5 μm), explaining the
248 greater number concentrations we simulate both at the surface and aloft. We also simulate
249 greater number concentration of fungal spores compared to Sesartic et al. (2013), at least
250 partly due to the greater emission flux we apply in our study. Our simulated zonal annual
251 mean number concentrations of fungal spores and bacteria are greatest in the lower
252 troposphere (number concentrations up to $1 \times 10^4 \text{ m}^{-3}$) decreasing to about 100 m^{-3} at 400 hPa.
253 Number concentrations of soot and dust are substantially larger, with annual zonal mean soot
254 and dust number concentrations as large as 1000 cm^{-3} and 1 cm^{-3} respectively in the NH
255 lower troposphere.

256 The low number concentrations of PBAP in comparison to other aerosol types, means that
257 both fungal spores and bacteria have little impact on global CCN concentrations. In our
258 simulations, bacteria increase global mean surface CCN concentrations (0.2%
259 supersaturation) by 0.01%. Including fungal spores in the model reduces global mean surface
260 CCN concentrations very slightly (by 0.001%) through a marginal suppression of nucleation.
261 Regionally, both bacteria and fungal spores alter CCN concentrations by less than 1% even
262 over tropical forest regions.

263 Figure 4 shows zonal annual mean all-sky immersion freezing rates for fungal spores,
264 bacteria, soot and dust. We find that global immersion freezing rates are dominated by dust
265 (96.4%) and soot (3.6%) with PBAP contributing only $1.4 \times 10^{-5}\%$. When we calculate
266 immersion freezing rates weighted by ice-cloud fraction, global annual mean rates are still
267 dominated by dust (97.2%) with smaller contributions from soot (2.8%), fungal spores
268 ($8.1 \times 10^{-6}\%$) and bacteria ($1.3 \times 10^{-6}\%$). Hoose et al. (2010a; b) also calculated a minimal
269 contribution from PBAP ($1.2 \times 10^{-5}\%$) with large contributions from dust (87.6%) and soot
270 (12.4%). The lower contribution from soot in our study is due to the lower absolute number
271 concentrations of soot that we simulate. We simulate a larger all-sky contribution from
272 PBAP ($3 \times 10^{-3}\%$) under the upper limit for IN formation from PBAP, but global rates are still
273 dominated by dust and soot.

274 Our simulated spatial pattern of immersion freezing rates is similar to that from previous
275 studies (e.g., Hoose et al., 2010b). Bacteria and fungal spore immersion freezing rates are
276 greatest in the lower troposphere at high latitudes and 400 hPa to 600 hPa in the tropics.
277 Immersion freezing rates of soot and dust are maximum at higher altitudes, being greatest at
278 400 hPa to 600 hPa at high latitudes and 400 hPa to 200 hPa in the tropics. Above 400 hPa,
279 immersion freezing rates of soot and dust are as large as $1 \times 10^{-6} \text{ cm}^{-3} \text{ s}^{-1}$, several orders of
280 magnitude greater than immersion freezing rates of either fungal spore or bacteria (1×10^{-14}
281 $\text{cm}^{-3} \text{ s}^{-1}$). However, at lower altitudes simulated immersion freezing rates of PBAP, dust and
282 soot are more comparable. Between 400hPa and 600 hPa, simulated freezing rates of fungal

283 spores and bacteria are as great as $1 \times 10^{-12} \text{ cm}^{-3} \text{ s}^{-1}$, greater than the freezing rates of soot or
284 dust at these altitudes. Dust and soot are known to be important IN at temperatures below
285 about -15°C , but their ability to nucleate ice at warmer temperatures is unclear (Murray et al.,
286 2012).

287 Figure 5 shows the contribution of PBAP (bacteria and fungal spores) to total all-sky zonal
288 annual mean immersion freezing rates. Above 400 hPa, PBAP contribute less than 0.001% to
289 zonal annual mean immersion freezing rates. At warmer temperatures, PBAP can make an
290 important contribution to zonal annual mean freezing rates with contribution to total freezing
291 rates reaching 100%.

292 To examine this behaviour in more detail, Figure 6 shows the contribution of PBAP to
293 immersion freezing rates at 260 K and 263 K in July 2000. Freezing rates are weighted by
294 ice-cloud fraction. At 263 K, PBAP, contributes ~20-100% of total immersion freezing rates
295 over most continental regions, with lower contribution over mostoceanic regions. At 260 K,
296 PBAP contributes typically 1-10% to total immersion freezing rates. We note that very small
297 immersion freezing rates at warmer temperatures may have limited atmospheric impacts.

298 **Discussion and Conclusions**

299 We have explored the contribution of fungal spores and bacteria to global aerosol number
300 concentrations. We included existing emission schemes for fungal spores and bacteria in a
301 global aerosol microphysics model. Simulated surface number concentrations of fungal
302 spores and bacteria were typically $2 \times 10^4 \text{ m}^{-3}$ over many continental regions. Simulated
303 number concentrations reasonably matched (typically within a factor 2) available
304 observations, although the model overpredicts fungal spore concentrations over forest
305 ecosystems and underpredicts bacteria number concentrations over grass, shrub and crop
306 ecosystems. A more detailed evaluation of the model is not possible because observations of
307 fungal spore and bacteria number are limited, are subject to methodological issues and rely
308 on counting techniques with inherent operator error. Long-term observations (longer than a
309 few weeks) of PBAP number are particularly scarce. New methods employing laser induced
310 fluorescence to identify and count biological particles (e.g., Gabey et al., 2010; 2011;
311 Huffman et al., 2010) may offer new opportunities to evaluate model predictions. We note
312 that existing PBAP emission schemes have not been designed to adequately represent
313 seasonal and interannual variability.

314 We found that fungal spores and bacteria contributed 8% and 5% respectively to global
315 continental mean supermicron number concentrations. Regionally, the contribution was
316 greater with fungal spores contributing 25% of supermicron number concentration over many
317 continental mid-latitude regions and up to 50% over tropical forests. The low number
318 concentrations of fungal spores and bacteria compared to other aerosol types results in a
319 limited contribution (<1%) of PBAP to regional CCN concentrations. It is important to note
320 that PBAP may be able to act as giant ($> 2 \mu\text{m}$) CCN (Möhler et al., 2007), something that we
321 did not study here.

322 We used an existing parametrization of immersion freezing rates (Hoose et al., 2010a; b) in
323 combination with our simulated aerosol number to quantify the contribution of PBAP to ice
324 nucleation. We found that fungal spores and bacteria contribute less than 3×10^{-3} % to global
325 all-sky immersion freezing rates, matching recent global model studies that find PBAP to be
326 unimportant as a source of IN at the global scale (Hoose et al., 2010a; b). We find a similarly
327 small contribution of PBAP to global immersion freezing rates when we weighted freezing
328 rates by ice cloud fraction. Although PBAP has little impact on global immersion freezing
329 rates, we found PBAP may be important at altitudes between 400 hPa and 600 hPa, where
330 warm temperatures ($> -15^{\circ}\text{C}$) inhibit the formation of ice from soot and dust. At these
331 altitudes, PBAP dominate immersion freezing rates in our simulations, matching case study
332 observations that recorded a large contribution of PBAP to IN formation (Christner et al.,
333 2008; Pratt et al., 2009; Prenni et al., 2009).

334 Whilst we acknowledge that the IN activity of fungal spores and bacteria is uncertain
335 (Murray et al., 2012; Hoose & Möhler, 2012), our study suggests that there are regions of the
336 atmosphere where biological particles contribute substantially to small ice nucleation rates,
337 motivating additional research on the role of PBAP as IN. Furthermore, recent studies have
338 suggested that PBAP emissions are related to rainfall and relative humidity (Huffman et al.,
339 2013; Schumacher et al., 2013; Prenni et al., 2013) creating daily variability in emissions not
340 accounted for here and potentially leading to tighter coupling between PBAP emissions and
341 climate.

342 **Acknowledgements**

343 This work was supported by the Natural Environment Research Council (NE/G015015/1) and
344 by the U.S. National Science Foundation (AGS-1238109).

345 **References**

346 Bauer, H., Giebl, H., Hitzenberger, R., Kasper-Giebl, A., Reischl, G., Zibuschka, F., and
347 Puxbaum, H.: Airborne bacteria as cloud condensation nuclei, *J. Geophys. Res.*, 108, 4658,
348 doi:10.1029/2003JD003545, 2003.

349
350 Bowers, R. M., Clements, N., Emerson, J. B., Wiedinmyer, C., Hannigan, M. P., and Fierer,
351 N.: Seasonal variability in bacterial and fungal diversity of the near surface atmosphere,
352 *Environ. Sc. Technol.*, 47, 12097-12106, 2013.

353
354 Burrows, S. M., Elbert, W., Lawrence, M. G., and Pöschl, U.: Bacteria in the global
355 atmosphere – Part 1: Review and synthesis of literature data for different ecosystems, *Atmos.*
356 *Chem. Phys.*, 9, 9263-9280, doi:10.5194/acp-9-9263-2009, 2009a.

357
358 Burrows, S. M., Butler, T., Jöckel, P., Tost, H., Kerkweg, A., Pöschl, U., and
359 Lawrence, M. G.: Bacteria in the global atmosphere – Part 2: Modeling of emissions and
360 transport between different ecosystems, *Atmos. Chem. Phys.*, 9, 9281-9297, doi:10.5194/acp-
361 9-9281-2009, 2009b.

362

363 Chipperfield, M. P. New version of the TOMCAT/SLIMCAT off-line chemical transport
364 model: Intercomparison of stratospheric tracer experiments, *Q. J. R. Meteorolo. Soc.*, 132,
365 1179-1203, 2006.

366

367 Christner, B. C., Morris, C. E., Foreman, C. M., Cai, R. M., and Sands, D. C.: Ubiquity of
368 biological ice nucleators in snowfall, *Science*, 319, 1214–1214, doi:10.1126/science.1149757,
369 2008.

370

371 DeLeon-Rodriguez, N., Latham, T. L., Luis M. Rodriguez-R, L. M., Barazesh, J. M.,
372 Anderson, B. E., Beyersdorf, A. J., Ziemba, L. D., Bergin, M., Nenes, A., and Konstantinidis,
373 K.T.: Microbiome of the upper troposphere: Species composition and prevalence, effects of
374 tropical storms, and atmospheric implications, *Proceedings of the National Academy of
375 Sciences of the United States of America*, doi:10.1073/pnas.1212089110, 2013.

376

377 Després, V.R. et al. Primary biological aerosol particles in the atmosphere: a review. *Tellus*
378 64B, 15598, doi:10.3402/tellusb.v6430.15598.

379

380 Elbert, W., Taylor, P. E., Andreae, M. O., Pöschl, U.: Contribution of fungi to primary
381 biogenic aerosols in the atmosphere: wet and dry discharged spores, carbohydrates, and
382 inorganic ions, *Atmos. Chem. Phys.*, 7, 4569-4588, 2007.

383

384 Gabey, A. M., Gallagher, M.W., Whitehead, J., Dorsey, J. R., Kaye, P. H., and Stanley, W.
385 R.: Measurements and comparison of primary biological aerosol above and below a tropical
386 forest canopy using a dual channel fluorescence spectrometer, *Atmos. Chem. Phys.*, 10,
387 4453–4466, doi:10.5194/acp-10-4453-2010, 2010.

388

389 Gabey, A. M., Stanley, W. R., Gallagher, M. W., and Kaye, P. H.: The fluorescence
390 properties of aerosol larger than 0.8 μm in urban and tropical rainforest locations, *Atmos.
391 Chem. Phys.*, 11, 5491-5504, doi:10.5194/acp-11-5491-2011, 2011.

392

393 Grinn-Gofron, A., Strzelczak, A., Wolski, T.: The relationship between air pollutants,
394 meteorological parameters and concentration of airborne fungal spores, *Environmental
395 Pollution*, 159, 602-608, 2011.

396

397 Hasnain, S. M., Akhter, T., Waqarm, M. A.: Airborne and allergenic fungal spores of the
398 Karachi environment and their correlation with meteorological factors, *J. Environ. Monit.*, 14
(1006), 2012.

399

400 Heald, C. L., and D. V. Spracklen (2009), Atmospheric budget of primary biological aerosol
401 particles from fungal spores, *Geophys. Res. Lett.*, 36, L09806, doi:10.1029/2009GL037493.

402

403 Henríquez, V. I., Villegas, G. R., Nolla, J. M. R.: Airborne fungi monitoring in Santiago,
404 Chile, *Aerobiologia*, 17, 137-142, 2001.

405

406 Herrero, A. D., Ruiz, S. S., Bustillo, M. G., Morales, P. C.: Study of airborne fungal spores in
407 Madrid, Spain, *Aerobiologia*, 22, 135-142, 2006.

408

409 Ho, H. M., Rao, C. Y., Hsu, H. H., Chiu, Y. H., Liu, C. M. and Chao, H. J.: Characteristics
410 and determinants of ambient fungal spores in Hualien, Taiwan, *Atmos. Environ.*, 39, 5839–
411 50, 2005.

412
413 Hoose, C., Kristjánsson, J. E., Burrows, S. M. How important is biological ice nucleation in
414 clouds on a global scale? *Environ. Res. Lett.* **5**, 2010a.

415 Hoose, C., Kristjánsson, J. E., Chen, J.-P., Harza, A. A classical-theory-based
416 parameterization of heterogeneous ice nucleation by mineral dust, soot, and biological
417 particles in a global climate model. *Journal of the Atmospheric Sciences* **67**, 2483-2503,
418 2010b.

419 Hoose, C. & Möhler, O.: Heterogeneous ice nucleation on atmospheric aerosols: a review of
420 results from laboratory experiments, *Atmos. Chem. Phys.*, **12**, 9817-9852, 2012.

421 Huffman, J. A., Treutlein, B., and Pöschl, U.: Fluorescent biological aerosol particle
422 concentrations and size distributions measured with an Ultraviolet Aerodynamic Particle
423 Sizer (UV-APS) in Central Europe, *Atmos. Chem. Phys.*, **10**, 3215-3233, doi:10.5194/acp-10-
424 3215-2010, 2010.

425 Huffman, J. A., Sinha, B., Garland, R. M., Snee-Pollmann, A., Gunthe, S. S., Artaxo, P.,
426 Martin, S. T., Andreae, M. O., and Pöschl, U.: Size distributions and temporal variations of
427 biological aerosol particles in the Amazon rainforest characterized by microscopy and real-
428 time UV-APS fluorescence techniques during AMAZE-08, *Atmos. Chem. Phys.*, **12**, 11997-
429 12019, doi:10.5194/acp-12-11997-2012, 2012.

430 Huffman, J. A., Prenni, A. J., DeMott, P. J., Pöhlker, C., Mason, R. H., Robinson, N. H.,
431 Fröhlich-Nowoisky, J., Tobo, Y., Després, V. R., Garcia, E., Gochis, D. J., Harris, E., Müller-
432 Germann, I., Ruzene, C., Schmer, B., Sinha, B., Day, D. A., Andreae, M. O., Jimenez, J. L.,
433 Gallagher, M., Kreidenweis, S. M., Bertram, A. K., and Pöschl, U.: High concentrations of
434 biological aerosol particles and ice nuclei during and after rain, *Atmos. Chem. Phys.*, **13**,
435 6151-6164, doi:10.5194/acp-13-6151-2013, 2013.

436 Jaenicke, R.: Abundance of cellular material and proteins in the atmosphere, *Science*, **308**,
437 73, 2005.

438 Jacobson, M. Z., and Streets, D. G.: Influence of future anthropogenic emissions on climate,
439 natural emissions and air quality, *J. Geophys. Res.*, **114**, D08118,
440 doi:10.1029/2008JD011476, 2009.

441 Lim, S. H., Chew, F. T., Dali, S. D. B. M., Tan, T. W., Lee, B. W., Tan, T. K.: Outdoor
442 airborne fungal spores in Singapore, *Grana*, **37** (4), 246-252, 1998.

443 Manktelow, P. T., Carslaw, K. S., Mann, G. W., and Spracklen, D. V.: The impact of dust on
444 sulfate aerosol, CN and CCN during an East Asian dust storm, *Atmos. Chem. Phys.*, **10**, 365-
445 382, doi:10.5194/acp-10-365-2010, 2010.

446 Mann, G. W., Carslaw, K. S., Spracklen, D. V., Ridley, D. A., Manktelow, P. T.,
447 Chipperfield, M. P., Pickering, S. J., and Johnson, C. E.: Description and evaluation of

448 GLOMAP-mode: a modal global aerosol microphysics model for the UKCA composition-
449 climate model, *Geosci. Model Dev.*, 3, 519-551, doi:10.5194/gmd-3-519-2010.

450 Mann, G. W. et al.: Intercomparison of modal sectional aerosol microphysics representations
451 within the same 3-D global chemical transport model, *Atmos. Chem. Phys.*, 12, 4449-4476,
452 2012.

453 Matthias-Maser, S. & Jaenicke, R.: The size distribution of primary biological aerosol
454 particles with radii $>0.2 \mu\text{m}$ in an urban rural influenced region, *Atmos. Res.*, 39, 279–286,
455 1995.

456
457 Matthias-Maser, S., Obolkin, V., Khodzer, T., & Jaenicke, R.: Seasonal variation of primary
458 biological aerosol particles in the remote continental region of Lake Baikal/Siberia,
459 *Atmospheric Environment* 34, 3805-3811, 2000.

460
461 Möhler, O., DeMott, P. J., Vali, G., and Levin, Z.: Microbiology and atmospheric processes:
462 the role of biological particles in cloud physics, *Biogeosciences*, 4, 1059-1071,
463 doi:10.5194/bg-4-1059-2007, 2007.

464
465 Murray, B. J., O’Sullivan, D., Atkinson, J. D., Webb, M. E.: Ice nucleation by particles
466 immersed in supercooled cloud droplets, *Chem. Soc. Rev.*, 41, 6519-6554, 2012.

467
468 Petters, M. D. and Kreidenweis, S. M.: A single parameter representation of hygroscopic
469 growth and cloud condensation nucleus activity, *Atmos. Chem. Phys.*, 7, 1961–1971,
470 doi:10.5194/acp-7-1961-2007, 2007.

471
472 Phillips, V. T. J., Andronache, C., Christner, B., Morris, C. E., Sands, D. C., Bansemer, A.,
473 Lauer, A., McNaughton, C., and Seman, C.: Potential impacts from biological aerosols on
474 ensembles of continental clouds simulated numerically, *Biogeosciences*, 6, 987-1014,
475 doi:10.5194/bg-6-987-2009, 2009.

476
477 Pöschl, U. et al. Rainforest aerosols as biogenic nuclei of cloud and precipitation in the
478 Amazon. *Science* 329, 1513, doi:10.1126/science.1191056, 2010.

479
480 Pratt, K. A., DeMott, P. J., French, J. R., Wang, Z., Westphal, D. L., Heymsfield, A. J.,
481 Twohy, C. H., Prenni, A. J. and Prather, K. A.: In situ detection of biological particles in
482 cloud ice-crystals. *Nat. Geosci.*, 2, 398–401, 2009.

483
484 Prenni, A. J., Petters, M. D., Kreidenweis, S. M., Heald, C. L., Martin, S. T., Artaxo, P.,
485 Garland, R. M., Wollny, A. G. and Pöschl, U. *Nat. Geosci.*, 2, 402–5, 2009.

486
487 Prenni, A. J., Tobo, Y., Garcia, E., DeMott, P. J., Huffman, J. A., McCluskey, C. S.,
488 Kreidenweis, S. M., Prenni, J. E., Pöhlker, C., Pöschl, U.: The impact of rain on ice nuclei
489 populations at a forested site in Colorado, *Geophys. Res. Lett.*, 40, 227–231,
490 doi:10.1029/2012GL053953, 2013.

491
492 Rossow, W. B. and Schiffer, R. A.: Advances in Understanding Clouds from ISCCP, *B. Am.*
493 *Meteorol. Soc.*, 80, 2261–2287, 1999.

494

495 Schumacher, C. J., Pöhlker, C., Aalto, P., Hiltunen, V., Petäjä, T., Kulmala, M., Pöschl, U.,
496 and Huffman, J. A.: Seasonal cycles of fluorescent biological aerosol particles in boreal and
497 semi-arid forests of Finland and Colorado, *Atmos. Chem. Phys. Discuss.*, 13, 17123-17158,
498 doi:10.5194/acpd-13-17123-2013, 2013.

499

500 Sesartic, A. and Dallafior, T. N. Global fungal spore emissions, review and synthesis of
501 literature data. *Biogeosciences* **8**, 1181-1192, 2011.

502

503 Sesartic, A., Lohmann, U., Storelvmo, T. Modelling the impact of fungal spore ice nuclei on
504 clouds and precipitation. *Environ. Res. Lett.* **8**, doi:10.1088/1748-9326/8/014029, 2013.

505

506 Sousa, S.I.V., et al., Corrigendum to “Influence of atmospheric ozone, PM10 and
507 meteorological factors on the concentration of airborne pollen and fungal spores”,
508 *Atmospheric Environment*, doi:10.1016/j.atmosenv.2008.06.052, 2009.

509

510 Spracklen, D. V., Pringle, K. J., Carslaw, K. S., Chipperfield, M. P., Mann, G. W.: A global
511 off-line model of size-resolved aerosol microphysics: I. Model development and prediction of
512 aerosol properties, *Atmos. Chem. Phys.*, 5, 2227-2252, 2005.

513

514 Tong, Y. Y. and Lighthart, B.: The annual bacterial particle concentration and size
515 distribution in the ambient atmosphere in a rural area of the Willamette valley, Oregon,
516 *Aerosol Sci. Technol.*, 32, 393–403, doi:10.1080/027868200303533, 2000.

517

518 Yttri, K. E., Simpson, D., Stenström, K., Puxbaum, H., and Svendby, T.: Source
519 apportionment of the carbonaceous aerosol in Norway – quantitative estimates based on 14C,
520 thermal-optical and organic tracer analysis, *Atmos. Chem. Phys.*, 11, 9375–9394, 2011.

521

522

523

524

525

526

527

528

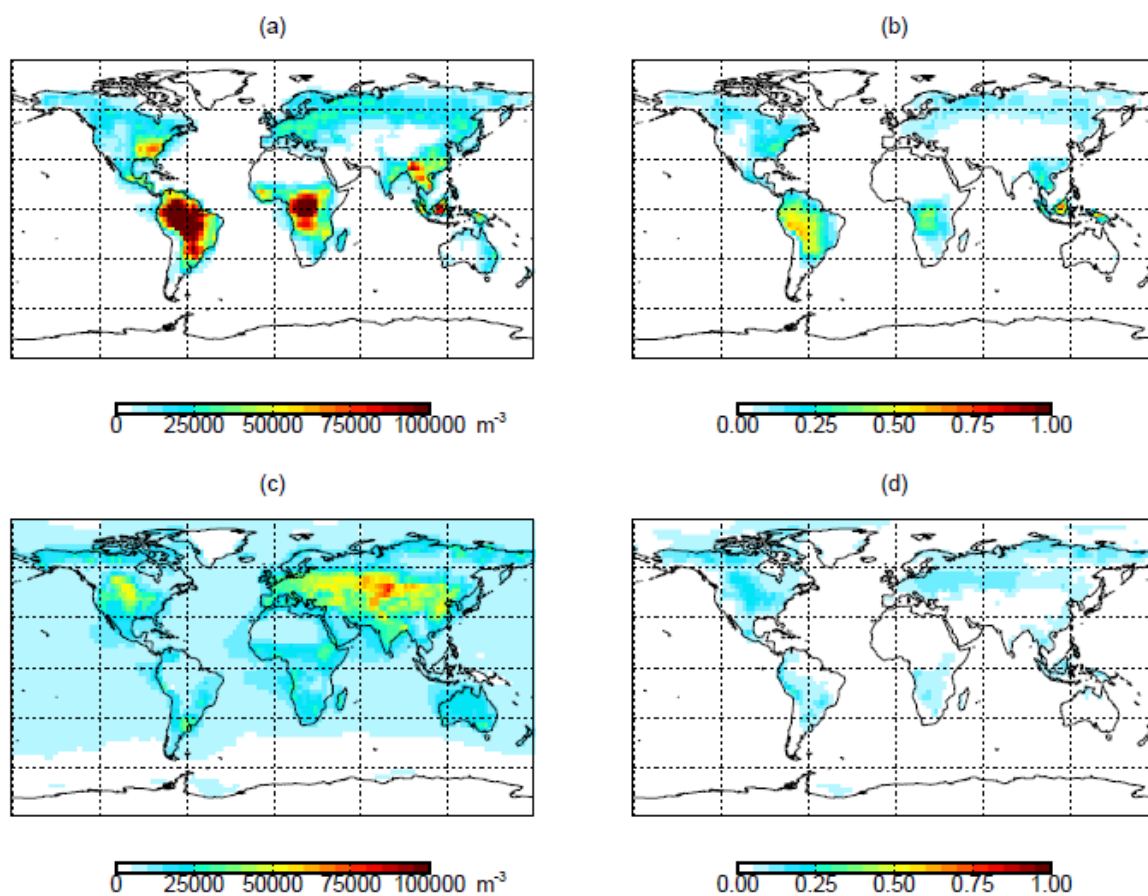
529

530

531

532

533



535

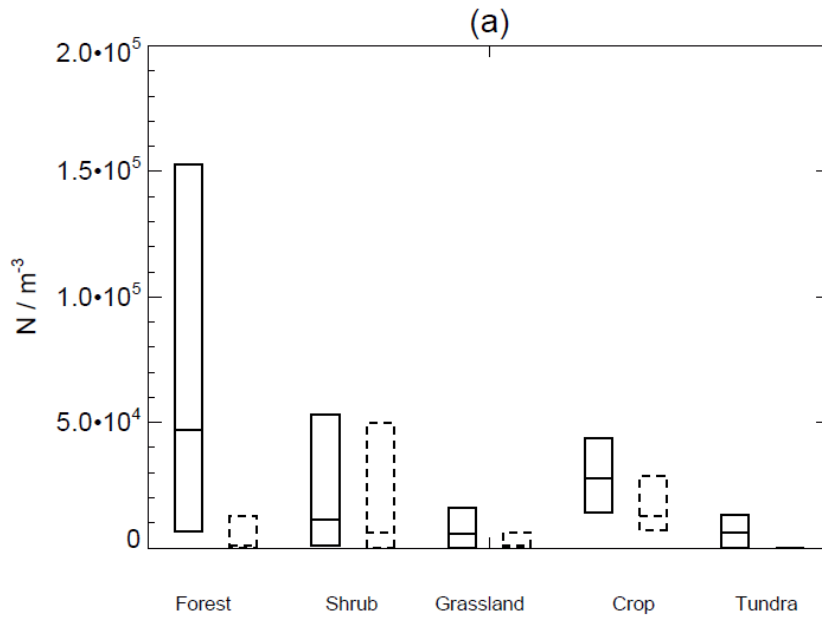
536 Figure 1. Simulated surface annual mean (a) fungal spore number concentrations, (b)
537 fractional contribution of fungal spores to supermicron surface number, (c) bacteria number
538 concentrations and (d) fractional contribution of bacteria to supermicron number
539 concentrations

540

541

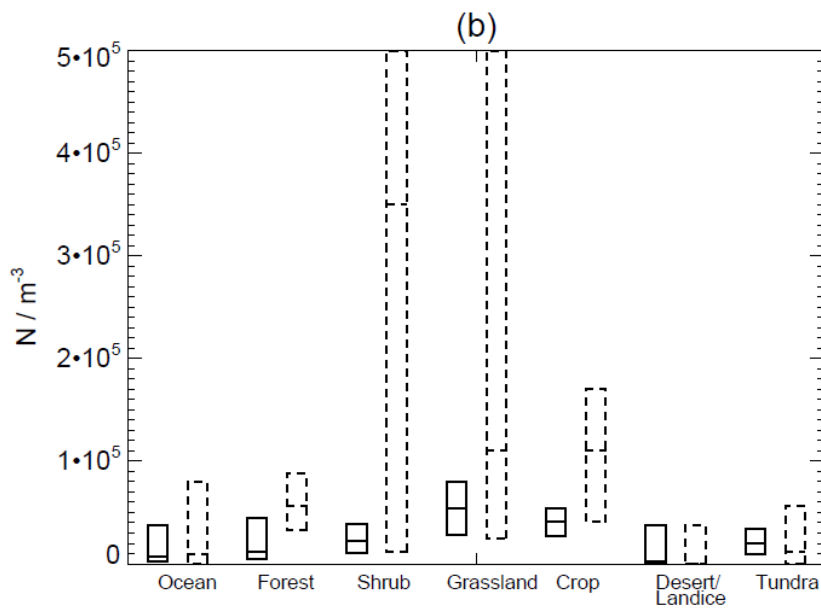
542

543



544

545

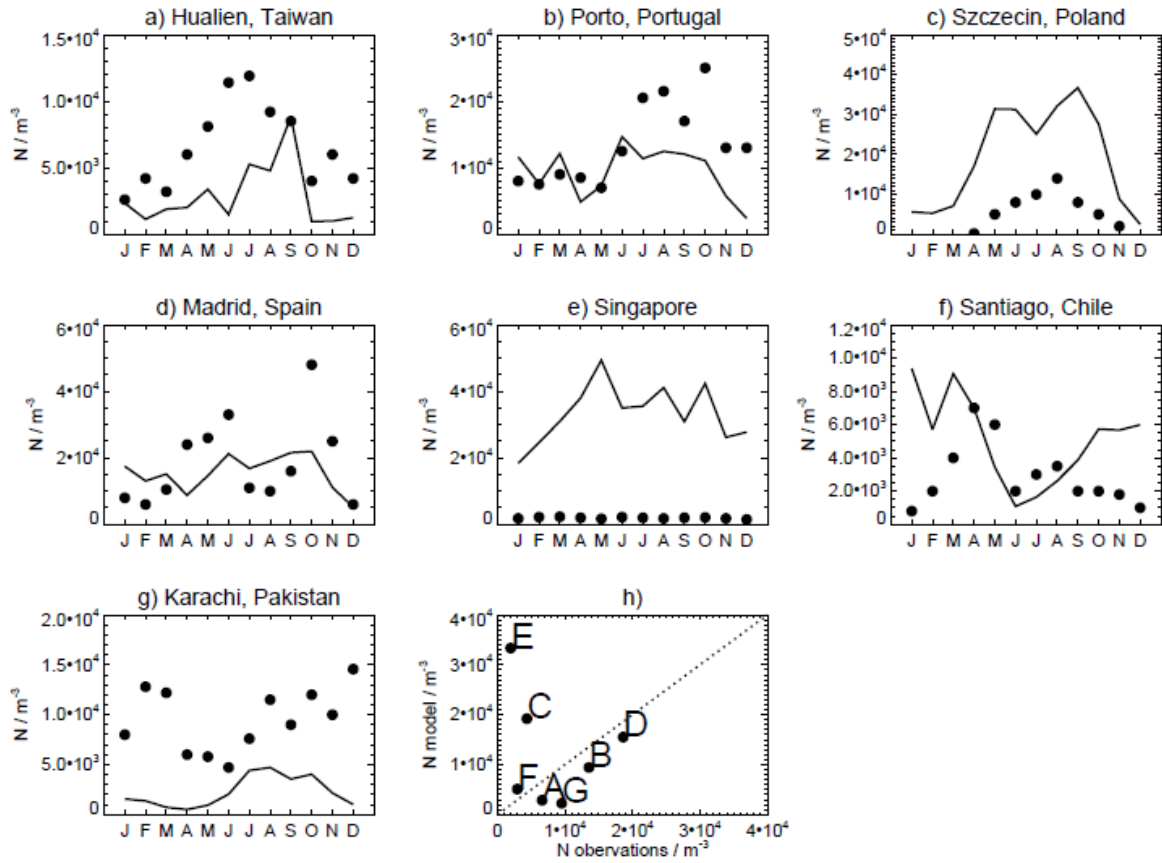


546

547 Figure 2. Comparison of simulated (solid) and observed (dashed) surface (a) fungal spore and
 548 (b) bacteria number concentrations across different ecosystems. Boxes show minimum, mean
 549 and maximum concentrations. Observed concentrations are a synthesis of total bacteria
 550 number concentrations in near surface air from Burrows et al. (2009a). The observed
 551 maximum for shrub and grasslands is $8.4 \times 10^4 \text{ m}^{-3}$ and extends off the scale. Simulated
 552 concentrations are the mean, maximum and minimum annual mean surface concentrations for
 553 that ecosystem type.

554

555



556

557 Figure 3. Evaluation of simulated fungal spore number concentrations. (a)-(g) Comparison of
 558 observed (circles) and simulated (black lines) monthly mean concentrations. (h) Comparison
 559 of simulated and observed annual mean concentrations. Observations are from Ho et al.,
 560 2005; Sousa et al., 2008; Grinn-Gofron et al., 2011; Herrero et al., 2006; Lim et al., 1998;
 561 Henriquez et al., 2001; Hasnain et al., 2012 respectively.

562

563

564

565

566

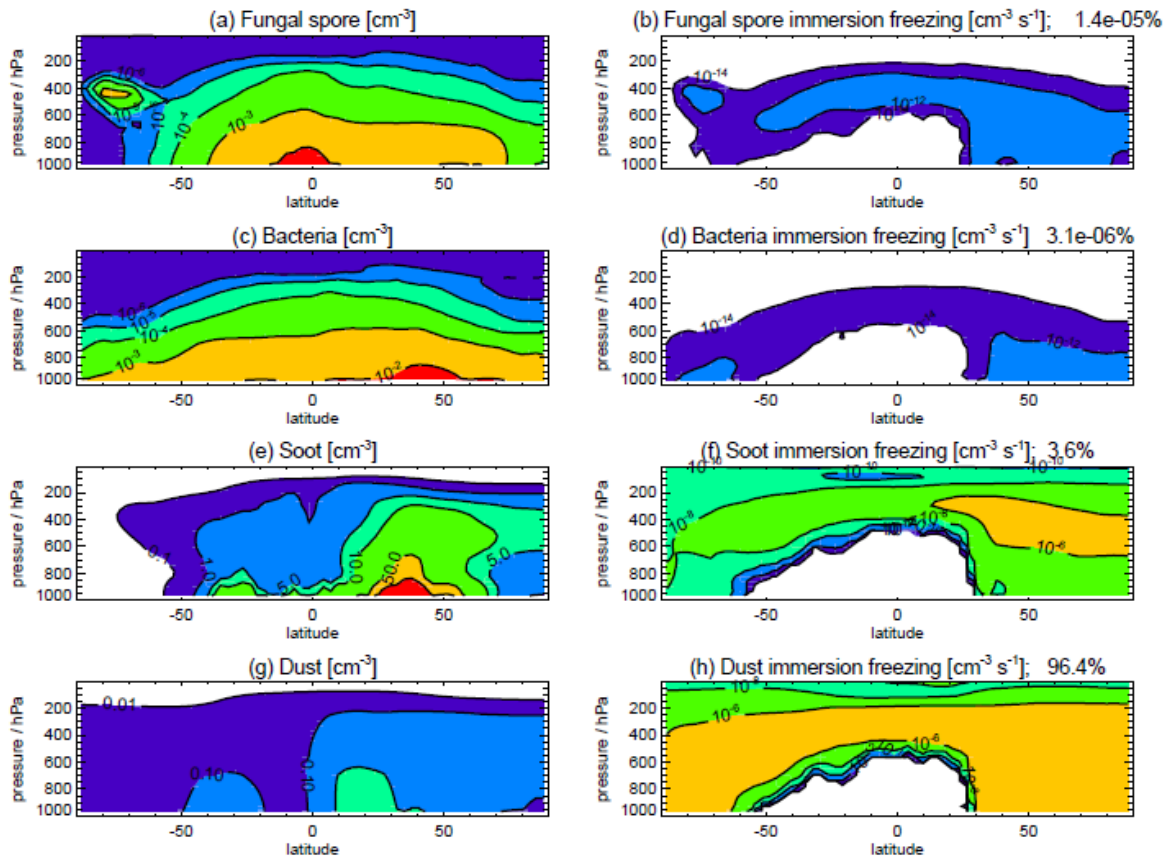
567

568

569

570

571



572

573 Figure 4. Zonal annual mean number concentrations for (a) fungal spores, (c) bacteria, (e)
 574 soot, (g) dust and all-sky immersion freezing rates for (b) fungal spores, (d) bacteria, (f) soot
 575 and (h) dust. Note (e) and (g) have a different colour scale to (a) and (c). Numbers above
 576 panel show percentage contribution to annual mean all-sky freezing rate. Weighting by ice-
 577 cloud fraction does not greatly change fractional contribution (see text).

578

579

580

581

582

583

584

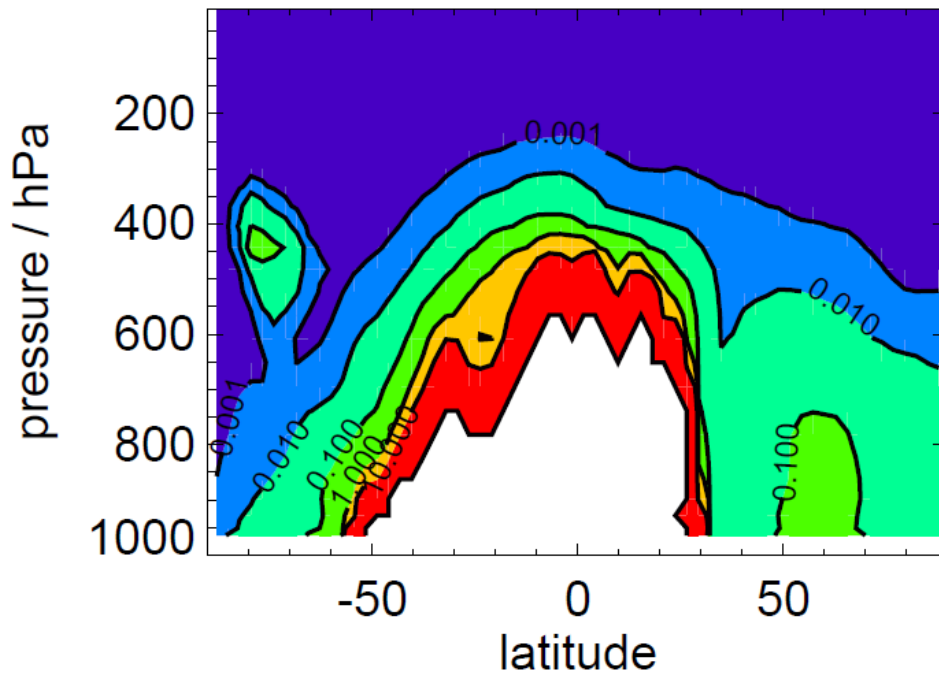
585

586

587

588

589



590

591 **Figure 5.** Percentage contribution of PBAP (bacteria and fungal spores) to zonal annual mean
592 all-sky immersion freezing rates. Values are for the upper limit contribution of PBAP to
593 immersion freezing (see text). White colour shows where total immersion freezing rate is less
594 than $1 \times 10^{-14} \text{ cm}^{-3} \text{ s}^{-1}$.

595

596

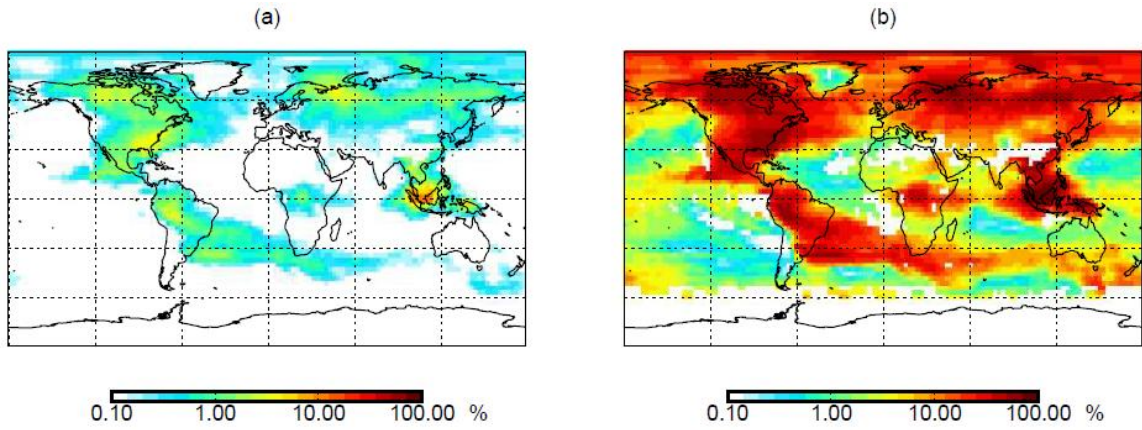
597

598

599

600

601



602 **Figure 6.** Percentage of immersion freezing simulated to be due to PBAP (bacteria and
603 fungal spores) in July 2000 at (a) 260 K and (b) 263 K. Values are for the upper limit
604 contribution of PBAP to immersion freezing and are weighted by ice cloud fraction (see text).
605

606

607

608

609

610

611

612

613

614

615

616

617

618

619

620

621

622

623